Journal of Materials Chemistry A

ROYAL SOCIETY OF CHEMISTRY

COMMUNICATION

Cite this: *J. Mater. Chem. A*, 2020, **8**, 5049

Received 24th November 2019
Accepted 31st January 2020

DOI: 10.1039/c9ta12889a

rsc.li/materials-a

Pressure effects on sulfide electrolytes for all solid-state batteries†

Jean-Marie Doux,[a] Yangyuchen Yang,[b] Darren H. S. Tan,[a] Han Nguyen,[a] Erik A. Wu,[a] Xuefeng Wang,[a] Abhik Banerjee[a] and Ying Shirley Meng *[abc]

All solid-state batteries are believed to be safer than their liquid counterparts owing to their use of nonflammable solid electrolytes. Nevertheless, unlike liquid electrolyte batteries, stack pressure is required during cycling to avoid contact losses between the electrodes and the solid electrolyte. Although recent studies have shown stack pressures to affect the capacity utilization of alloying anodes, an investigation of the effect of stack pressures on solid-state battery cyclability has not been performed so far. In this work, the effects of both initial fabrication pressure and operating stack pressure on the electrolyte's ionic conductivity and battery performance have been analyzed; the results show that initial fabrication pressure directly affects the porosity of the electrolyte and therefore the overall performance of the cell. Low operating stack pressure reduces the apparent ionic conductivity due to poor contact between the electrolyte and current collectors, but does not detrimentally affect the cyclability of solid-state batteries. These results can explain inconsistencies in the literature and provide a guideline toward standardized solid-state battery testing conditions and proper reporting benchmarks of the performance of solid-state batteries.

Introduction

All solid-state batteries (ASSBs) are expected to revolutionize the Li-ion battery landscape thanks to several advantages: the use of non-flammable electrolytes which improves their intrinsic safety and their potential to enable metallic Li anodes, allowing for a substantial increase in energy density. While stack pressure is deemed necessary to ensure proper contact of electrodes with the solid-electrolyte and also inhibit delamination during cycling due to electrode expansion and contraction,[1–5] there are no reports thus far of how stack pressure affects the performance of all solid-state batteries. Most literature reports today use solid-state cells designed to apply uniaxial stack pressure, the value of which is often not mentioned or is approximative.[6,7] Nevertheless, stack pressure has been shown to strongly influence the capacity of alloying anodes,[8] the electrochemical stability window of solid electrolytes,[9] and even the cyclability of lithium metal in ASSBs.[10,11] It is necessary to understand the effect of stack pressure on solid-state batteries to allow for proper experimental design and optimization of performance parameters.

In contrast, the pressure used to fabricate a sulfide solid-state electrolyte pellet (by cold-pressing) has been widely reported by the scientific community, as it directly affects the porosity of the electrolyte. Studies have already shown that a lower fabrication pressure (which results in higher porosity) reduces the apparent ionic conductivity of the electrolyte.[12,13] However, the effect of operating stack pressure on this ionic conductivity also needs to be characterized.[14,15] This may explain the large differences in electrochemical measurements in the literature for the same solid electrolyte material.

In this work, we designed a solid-state battery holder with a load cell that allows accurate control of the stack pressure. From this, the effect of both the fabrication and the stack pressure has been studied at the electrolyte and at the half cell level using a $LiNbO_3$-coated $LiNi_{0.80}Co_{0.15}Al_{0.05}O_2$ (LNO-NCA)|Li_6PS_5Cl (LPSCl)|Li–In alloy solid-state battery. First, we show that fabrication pressure has a direct impact on the solid electrolyte pellet porosity, as confirmed by the focused ion beam (FIB) 3D reconstruction. Once sufficiently high fabrication pressure is achieved, the relative density of the pellet no longer increases, and the ionic conductivity attains its maximal value. At lower fabrication pressures, the lower electrolyte density reduces the measured ionic conductivity of the electrolyte. This lower conductivity has a negative impact on the cyclability and rate capability of the all solid-state battery. Secondly, we found

[a]*Department of Nano Engineering, University of California San Diego, La Jolla, CA 92093, USA. E-mail: shirleymeng@ucsd.edu*

[b]*Materials Science and Engineering, University of California San Diego, La Jolla, CA 92093, USA*

[c]*Sustainable Power & Energy Center (SPEC), University of California San Diego, La Jolla, CA 92093, USA*

† Electronic supplementary information (ESI) available. See DOI: 10.1039/c9ta12889a

that the operating stack pressure has a negligible impact on the electrolyte conductivity as long as good contact between the electrolyte and the current collector is established, which can be achieved by using a soft material such as carbon powder. Similarly, the all solid-state battery performance is not affected by the operating stack pressure as the electrodes already have good electronic contact with the current collector.

Discussion

With reference to Table 1 summarizing the literature reports on the ionic conductivity of argyrodite Li_6PS_5Cl, large discrepancies can be noticed. While some of these variations could easily be explained by slight differences in room temperature conditions during the conductivity measurement, some values differ by as much as two orders of magnitude. Upon closer examination, it appears that the solid-state sulfide electrolyte is densified by cold pressing at widely different fabrication pressures in each report. As the fabrication pressure has a direct effect on the electrolyte's porosity, larger contributions from the grain boundaries are expected at a lower fabrication pressure and, therefore, a lower ionic conductivity.[28,29] This large variation in fabrication pressure can likely explain some of the discrepancies between these reported conductivity values, as can the presence of impurities, degree of crystallinity/amorphization of the material, particle size (influencing the densification process), and so on.[28] Nevertheless, while typical parameters such as fabrication pressure and current collector material (from stainless steel to carbon powder to silver paste) are often reported, there is no mention of the operating stack pressure used during the conductivity measurement so far. In order to determine the most suitable protocol to measure and report the conductivity of sulfide solid-state electrolytes, the influence of these parameters must be studied.

Fig. 1a describes the experimental setup used to measure the applied stack pressure during electrochemical measurements. The solid-state battery is built inside a polyether ether ketone (PEEK) pellet mold using titanium plungers that double as current collectors. The assembly is then placed in a cell holder on which a controlled stack pressure is applied by tightening the nuts on the three bolts. PEEK insulating discs prevent an external short circuit of the cell through the metallic holder. A load cell connected to a calibrated digital meter (in MPa using a materials test frame) provides an accurate reading of the stack pressure during cycling. The effects of two different pressures on the conductivity of the solid-state sulfide electrolyte and on the cycling performance of the all solid-state battery were investigated: the fabrication pressure and the operating stack pressure.

Fig. 2a shows the conductivity of the Li_6PS_5Cl electrolyte as a function of the operating stack pressure, using titanium plungers or carbon powder as the current collector. When using the titanium current collector, it appears that a low stack pressure induces a large contact impedance which is reflected in the low ionic conductivity value: at 2 MPa, the conductivity is only 0.2 mS cm^{-1} whereas it exceeds 2.0 mS cm^{-1} at 70 MPa. Hysteresis can also be observed: after releasing the stack pressure from 70 MPa, the conductivity at lower pressures is significantly higher than before. These observations show that the contact interface between the soft sulfide electrolyte and the hard titanium plunger depends strongly on the stack pressure. To avoid this, it is possible to use carbon powder as the current collector as it will conform to the surface and provide an electronically conductive interface. When using carbon, the ionic conductivity becomes almost independent of the applied stack pressure, ensuring a reliable measurement of the electrolyte's performance. These results suggest that most discrepancies in the literature on the conductivity of the argyrodite LPSCl electrolyte can be explained by the differences in the current collector and the stack pressure used. Similar results have also been obtained for the $Li_7P_3S_{11}$ solid-state electrolyte; the ionic conductivity varies between 10^{-4} and 10^{-3} S cm^{-1} as shown in Fig. S1 of the ESI.† It is expected that this contact impedance can be seen for most Li and Na sulfide solid-state electrolytes and therefore it is recommended to use carbon powder as the electrodes when measuring the electrolyte ionic conductivity.

With cycling solid-state batteries, the electrodes are usually relatively soft; Li metal or Li–In alloy anodes are ductile

Table 1 Conductivity of the argyrodite Li_6PS_5Cl solid-state electrolyte as reported in the literature. The fabrication pressure, stack pressure and electrode material are given where reported

Conductivity (mS cm^{-1})	Fabrication pressure (MPa)	Stack pressure (MPa)	Electrodes	Reference
0.22–3.02	**50–370**	**5–70**	**Carbon–titanium**	**This work**
4.96	1000	—	Stainless steel	16
1.33	333	—	Carbon	17
0.74	—	—	Stainless steel	18
1.40	360	—	—	19
3.15	150	—	Stainless steel	20
1.10	750	—	Stainless steel	21
1.90	—	—	Stainless steel	22
0.06	360	—	Stainless steel	23
0.28	—	—	Ag paste	24
1.60	330	—	Stainless steel	25
1.40	140	—	Stainless steel	26
1.29	350	—	—	27

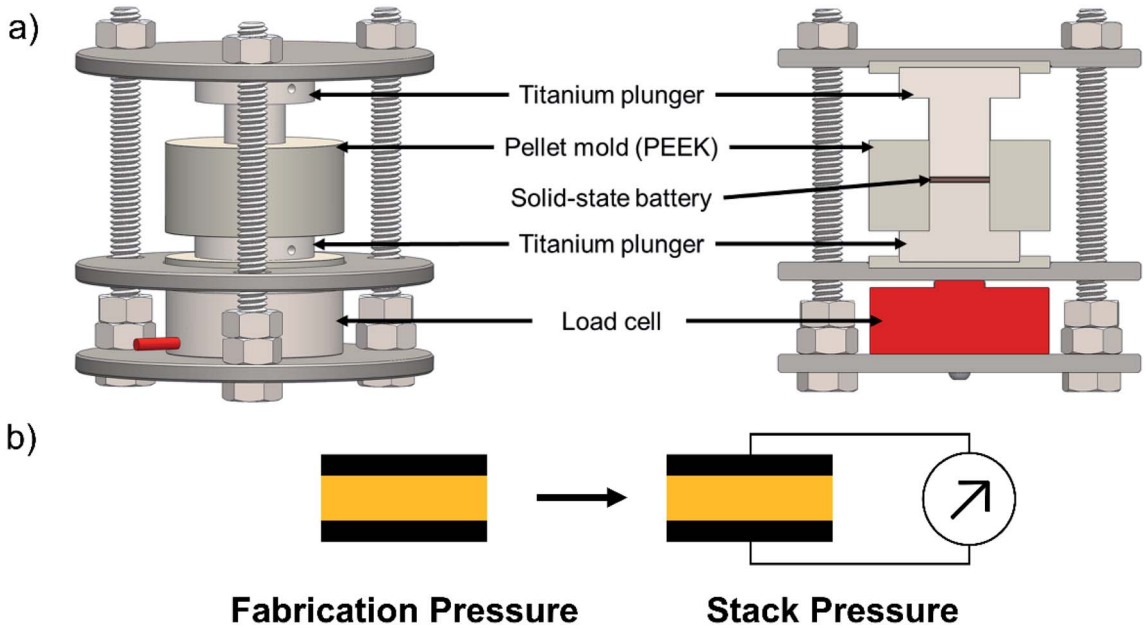

Fig. 1 (a) Design of the solid-state battery holder with a load cell to monitor the stack pressure applied to the battery during cycling and conductivity measurements. (b) For conductivity measurements and battery cycling, pellets are first prepared by applying uniaxial pressure as the fabrication pressure using a hydraulic press and are then cycled in the battery holder at the predetermined stack pressure.

materials, and anode/cathode composites are prepared in part with a sulfide solid-state electrolyte and carbon powder, also soft materials. Therefore, based on these results on the electrolyte conductivity, we can expect the influence of operating stack pressure on the cycling performance in solid-state batteries to be negligible. Fig. 2b shows the room-temperature cycling stability of two similar Li–In|LPSCl|LNO-coated NCA all solid-state batteries. LNO coating was used on the NCA cathode as it has been shown to prevent it from reacting with the electrolyte during cycling.[30] The first one has been cycled under a constant stack pressure of 25 MPa whereas for the second one, the stack pressure was increased every 5 cycles between 5 and 125 MPa and then released to 5 MPa. As expected, due to the softer electrode materials, the stack pressure does not have a distinguishable effect on the cycling stability of the cell. These experiments also allowed us to determine that further investigation of the fabrication pressure effect can be carried out using a generic constant stack pressure of 25 MPa.

Fig. 3a presents the evolution of the relative density of Li_6PS_5Cl pellets and their ionic conductivity (as determined by electrochemical impedance spectroscopy as shown in Fig. 3b) as a function of the fabrication pressure used to densify the electrolyte material. When increasing the fabrication pressure from 50 to 250 MPa, the relative density increases from 68.3 to 75.4%

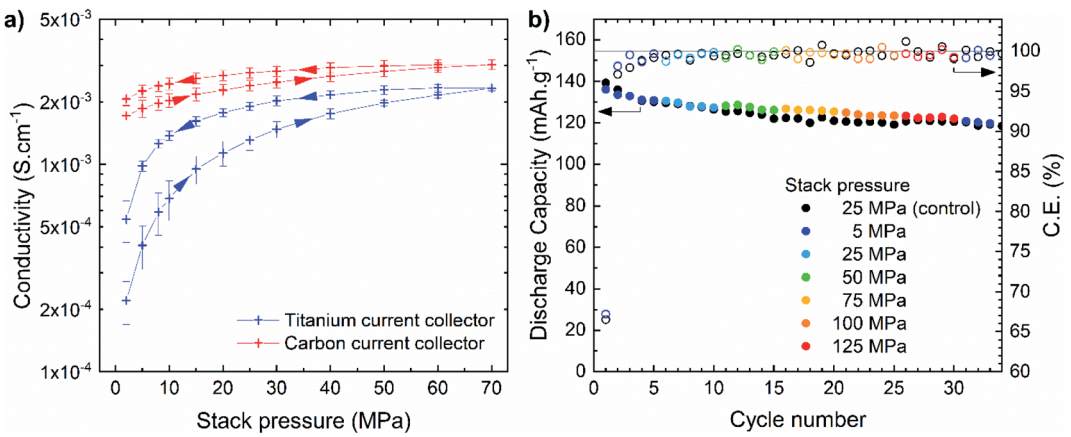

Fig. 2 (a) Conductivity of Li_6PS_5Cl as a function of the stack pressure using titanium plungers or pressed carbon powder as electrodes. The stack pressure was increased to 70 MPa and subsequently decreased to 5 MPa (as indicated by the arrows). Error bars represent the standard deviation of 4 samples. (b) Effect of stack pressure on the cycling stability (at room temperature) of Li|In|LPSCl|NCA solid-state batteries. Each pellet of the electrolyte and batteries was prepared using a fabrication pressure of 370 MPa.

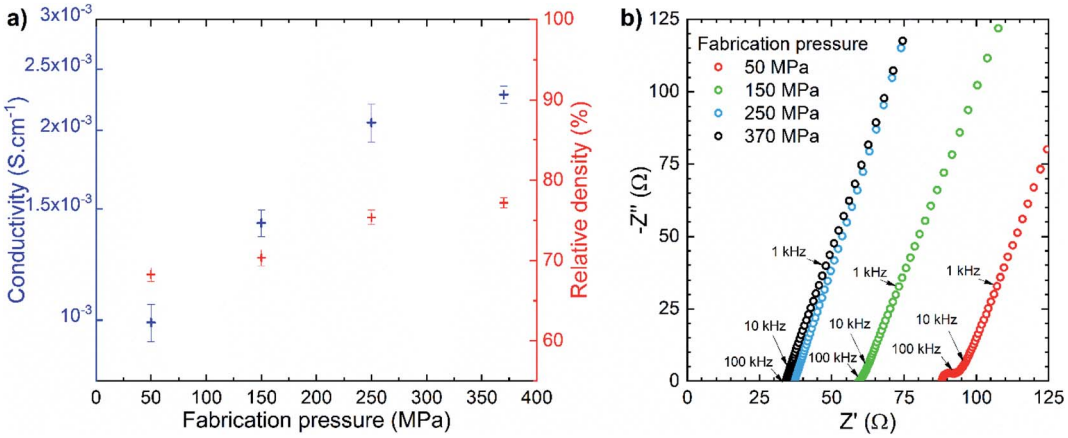

Fig. 3 (a) Conductivity and relative density of the Li_6PS_5Cl electrolyte as a function of the fabrication pressure and (b) Nyquist diagrams of the electrochemical impedance spectra at the same fabrication pressures. All measurements were performed with a stack pressure of 25 MPa. Error bars represent the standard deviation of 4 samples.

and the ionic conductivity shows a similar trend, increasing from 0.99 mS cm^{-1} to 2.06 mS cm^{-1}. Further increasing the fabrication pressure has a progressively smaller impact on the relative density of the pellet and therefore a limited effect on the ionic conductivity; 2.28 mS cm^{-1} is obtained at 370 MPa. These results confirm that the relative density – and therefore the porosity – of the solid-state electrolyte also influences the measured ionic conductivity. The Nyquist diagrams (Fig. 3b) show that at a lower fabrication pressure, the appearance of a semicircle in the high-frequency region can be attributed to

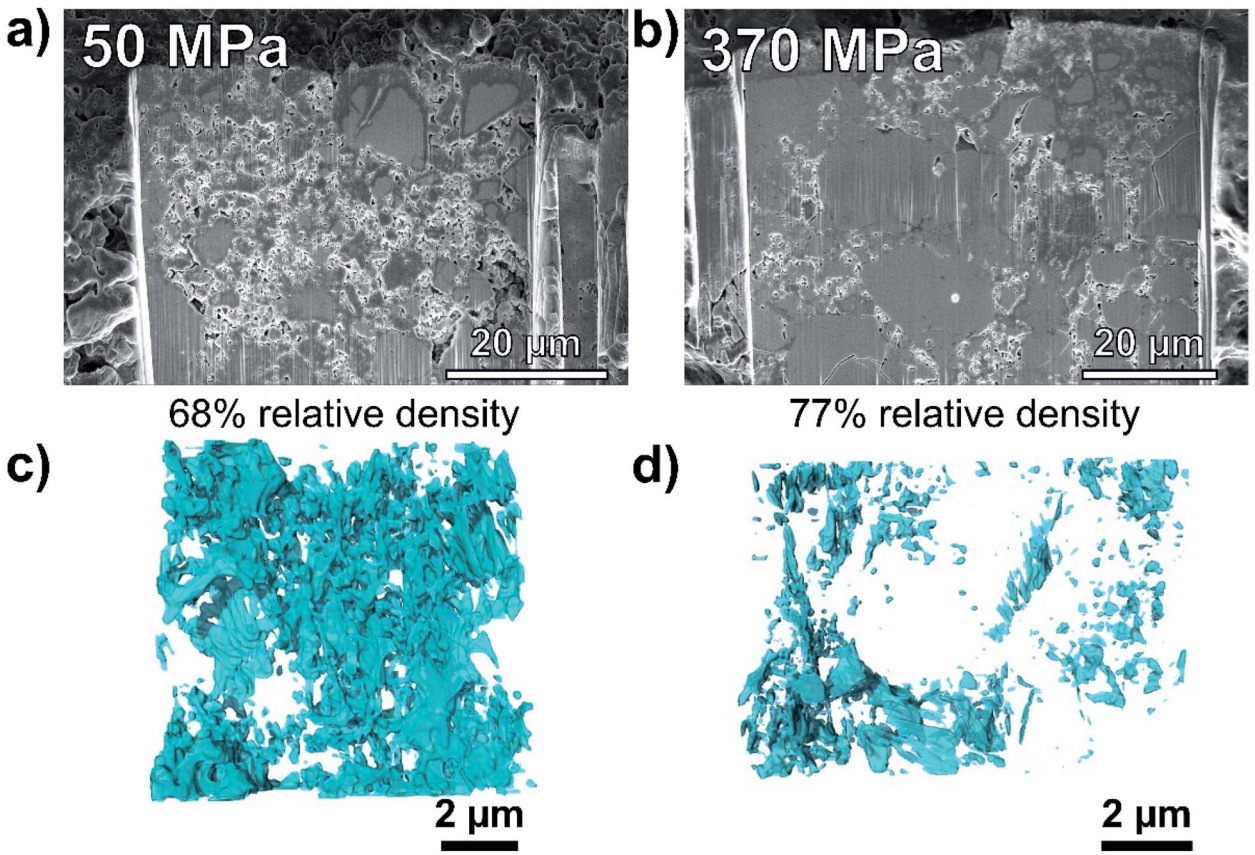

Fig. 4 SEM images of FIB cross-sections of Li_6PS_5Cl electrolyte pellets prepared with a fabrication pressure of (a) 50 MPa and (b) 370 MPa, with their corresponding relative densities estimated by physical measurements. The resulting FIB reconstructions show the porosity in blue for the (c) 50 MPa pellet and (d) 370 MPa pellet.

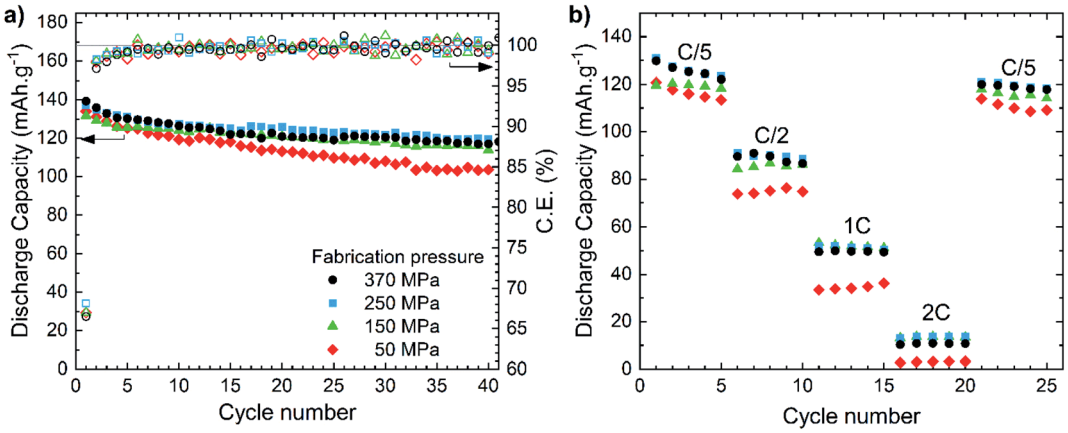

Fig. 5 (a) Cycling stability at C/10 and (b) rate performance as a function of the fabrication pressure of LiIn|LPSCl|NCA solid-state batteries. All these cells were cycled at room temperature at a stack pressure of 25 MPa.

the contribution of grain boundaries to the impedance of the system. As fabrication pressure increases, this contribution is reduced and cannot be identified anymore when the fabrication pressure exceeds 250 MPa. For oxide solid-state electrolytes, similar behavior is usually seen; increasing the relative density of the pellet by sintering reduces the grain boundary contribution and therefore increases the ionic conductivity.[28,29] In the case of sulfide electrolytes, the grain boundaries nevertheless have a high ionic conductivity compared to oxides,[31] as even with a porosity of more than 30%, LPSCl still exhibits an ionic conductivity higher than 1 mS cm^{-1}. For oxide electrolyte materials on the other hand, a relative density higher than 90% is usually sought after, as the grain boundary impedance is much higher; even an increase of 10% in the porosity can lower ionic conductivities by an order of magnitude.[32]

Fig. 4 shows the room-temperature cross-sectional SEM images and FIB 3D reconstructions of the void distribution of the LPSCl pellets densified at fabrication pressures of 50 MPa (Fig. 4a and c) and 370 MPa (Fig. 4b and d), respectively. The cross-sectional images clearly show a higher quantity of small grains at 50 MPa, indicating that the densification is not complete; in addition, some large pores can also be seen. On the other hand, the pellet densified at 370 MPa appears denser and made of larger grains. As a cross-sectional view is not representative of the volume distribution of the porosity, FIB 3D reconstruction was performed. While a large number of interconnected voids can be seen for the 50 MPa pellet, the porosity of the 370 MPa pellet is lower as the grains are bigger. This physical observation of the porosity confirms the resistive contribution of the grain boundaries observed by EIS. For comparison, FIB cross-sectional SEM was also performed at cryogenic temperatures for the pellet pressed at 370 MPa and the image is shown in Fig. S3.† The image confirms that no beam damage or degradation occurs during ion milling and imaging at room temperature.

The cycling stability at C/10 at room temperature of four similar solid-state batteries, built using fabrication pressures of 50, 150, 250 and 370 MPa, is shown in Fig. 5a. The cycling performances of the three cells fabricated at 150, 250 and 370 MPa are similar, with no distinguishable differences in Coulombic efficiency or discharge capacity over 40 cycles. The cell prepared with a fabrication pressure of 50 MPa, on the other hand, shows a significantly lower specific capacity after 40 cycles: only 103 mA h g^{-1} compared to around 115 mA h g^{-1} for the three other batteries. This indicates that the higher electrolyte impedance due to the low fabrication pressure has a direct impact on the cycling stability of the cell. This higher impedance also has a negative effect on the rate performance of the solid-state battery: as shown in Fig. 5b, the cell prepared with a fabrication pressure of 50 MPa shows much lower specific capacities at high rates. At a rate of 2C, this cell shows almost no capacity whereas the three other cells (150, 250 and 370 MPa) still exhibit capacities around 10 and 15 mA h g^{-1}. These experiments show that the fabrication pressure – and hence the densification of the electrolyte – is critical for the cell performance. It is therefore necessary to focus on reducing the porosity of the electrolyte layer, which can be achieved by improving the particle size distribution by using hot pressing or spark plasma sintering.[33,34]

The approach of using a high initial fabrication pressure followed by low operating stack pressure can be further extended to ASSBs in larger formats. As ASSBs manufactured in pouch formats can potentially reach areal sizes between 30 and 300 cm^2 or more,[35,36] the large uniaxial forces needed to maintain constant high stack pressures during operation make them mechanically impractical. From our earlier discussions, it can be concluded that high pressures are only necessary during cell fabrication, which can be achieved in large formats using hot roll-to-roll processing instead of the areal pressure applied in laboratory scale cells. Once the ideal relative densities are achieved in each electrode/electrolyte layer, large format type cells can then be operated under relatively low stack pressures without compromising the cell performance.[35,37]

Conclusion

In this work, the effect of fabrication pressure and operating stack pressure on the performance of solid-state electrolyte and batteries was investigated. The inconsistencies seen in the

literature in the ionic conductivity of Li_6PS_5Cl can be explained by the differences in operating stack pressure and the material used as electrodes for EIS measurements: using carbon powder shows an increase in the ionic conductivity of approximately one order of magnitude compared to solely using titanium plungers at the same stack pressure. A similar behavior is expected in most sulfide electrolytes and it is recommended to use carbon electrodes when evaluating the electrolyte conductivity to minimize the contact impedance. For solid-state batteries, since the fabrication pressure was shown to influence the electrolyte porosity, the fabrication pressure also has a large impact on cycling stability and rate performance of the cell. At a lower fabrication pressure (50 MPa), the significantly higher porosity generates more grain boundary impedance which is detrimental to the cell performance; the capacity retention and rate capability are significantly improved in ASSBs prepared at a high fabrication pressure (370 MPa). On the other hand, the operating stack pressure does not have a major influence on cycling stability, showing that it is possible to cycle sulfide based ASSBs at a reasonably low stack pressure without the need for complex or bulky housing materials. We believe these results allow for a better understanding of pressure effects on cell performance and emphasize the importance of reporting the operating stack pressure used, in order by the scientific community to standardize testing protocols in sulfide-based all solid-state batteries.

Conflicts of interest

There are no conflicts of interest to declare.

Acknowledgements

The authors would like to acknowledge the financial support received for this study from the LG Chem company through the Battery Innovation Contest (BIC) program. Part of this work was performed at the San Diego Nanotechnology Infrastructure (SDNI) of the UCSD, a member of the National Nanotechnology Coordinated Infrastructure, supported by the National Science Foundation (grant ECCS-1542148).

References

1 F. Hao, F. Han, Y. Liang, C. Wang and Y. Yao, *MRS Bull.*, 2018, **43**, 775–781.
2 T. Famprikis, P. Canepa, J. A. Dawson, M. S. Islam and C. Masquelier, *Nat. Mater.*, 2019, **18**, 1278–1291.
3 J. Janek and W. G. Zeier, *Nat. Energy*, 2016, **1**, 16141.
4 W. Zhang, D. Schröder, T. Arlt, I. Manke, R. Koerver, R. Pinedo, D. A. Weber, J. Sann, W. G. Zeier and J. Janek, *J. Mater. Chem. A*, 2017, **5**, 9929–9936.
5 J. Cannarella and C. B. Arnold, *J. Power Sources*, 2014, **245**, 745–751.
6 R. Koerver, F. Walther, I. Aygün, J. Sann, C. Dietrich, W. G. Zeier and J. Janek, *J. Mater. Chem. A*, 2017, **5**, 22750–22760.
7 X. Wu, M. El Kazzi and C. Villevieille, *J. Electroceram.*, 2017, **38**, 207–214.
8 D. M. Piper, T. A. Yersak and S.-H. Lee, *J. Electrochem. Soc.*, 2013, **160**, A77–A81.
9 W. Fitzhugh, L. Ye and X. Li, *J. Mater. Chem. A*, 2019, **7**, 23604–23627.
10 J.-M. Doux, H. Nguyen, D. H. S. Tan, A. Banerjee, X. Wang, E. A. Wu, C. Jo, H. Yang and Y. S. Meng, *Adv. Energy Mater.*, 2020, **10**, 1903253.
11 M. J. Wang, R. Choudhury and J. Sakamoto, *Joule*, 2019, **3**, 2165–2178.
12 A. Sakuda, A. Hayashi and M. Tatsumisago, *Sci. Rep.*, 2013, **3**, 2261.
13 A. Hayashi, A. Sakuda and M. Tatsumisago, *Front. Energy Res.*, 2016, **4**, 25.
14 F. Wu, W. Fitzhugh, L. Ye, J. Ning and X. Li, *Nat. Commun.*, 2018, **9**, 4037.
15 N. Riphaus, B. Stiaszny, H. Beyer, S. Indris, H. A. Gasteiger and S. J. Sedlmaier, *J. Electrochem. Soc.*, 2019, **166**, A975–A983.
16 C. Yu, S. Ganapathy, J. Hageman, L. van Eijck, E. R. H. van Eck, L. Zhang, T. Schwietert, S. Basak, E. M. Kelder and M. Wagemaker, *ACS Appl. Mater. Interfaces*, 2018, **10**, 33296–33306.
17 S. Boulineau, M. Courty, J.-M. Tarascon and V. Viallet, *Solid State Ionics*, 2012, **221**, 1–5.
18 P. R. Rayavarapu, N. Sharma, V. K. Peterson and S. Adams, *J. Solid State Electrochem.*, 2012, **16**, 1807–1813.
19 S. Yubuchi, S. Teragawa, K. Aso, K. Tadanaga, A. Hayashi and M. Tatsumisago, *J. Power Sources*, 2015, **293**, 941–945.
20 S. Wang, Y. Zhang, X. Zhang, T. Liu, Y.-H. Lin, Y. Shen, L. Li and C.-W. Nan, *ACS Appl. Mater. Interfaces*, 2018, **10**, 42279–42285.
21 C. Yu, L. van Eijck, S. Ganapathy and M. Wagemaker, *Electrochim. Acta*, 2016, **215**, 93–99.
22 R. P. Rao and S. Adams, *Phys. Status Solidi A*, 2011, **208**, 1804–1807.
23 N. C. Rosero-Navarro, A. Miura and K. Tadanaga, *J. Sol-Gel Sci. Technol.*, 2019, **89**, 303–309.
24 M. Xuan, W. Xiao, H. Xu, Y. Shen, Z. Li, S. Zhang, Z. Wang and G. Shao, *J. Mater. Chem. A*, 2018, **6**, 19231–19240.
25 A. Hwang, Y. Ma, Y. Cao, Q. Li, L. Wang, X. Cheng, P. Zuo, C. Du, Y. Gao and G. Yin, *Int. J. Electrochem. Sci.*, 2017, **12**, 7795–7806.
26 S. Choi, J. Ann, J. Do, S. Lim, C. Park and D. Shin, *J. Electrochem. Soc.*, 2019, **166**, A5193–A5200.
27 J. Zhang, H. Zhong, C. Zheng, Y. Xia, C. Liang, H. Huang, Y. Gan, X. Tao and W. Zhang, *J. Power Sources*, 2018, **391**, 73–79.
28 D. Pérez-Coll, E. Sánchez-López and G. C. Mather, *Solid State Ionics*, 2010, **181**, 1033–1042.
29 J.-M. Doux, L. Leguay, A. Le Gal La Salle, O. Joubert and E. Quarez, *Solid State Ionics*, 2018, **324**, 260–266.
30 A. Banerjee, H. Tang, X. Wang, J.-H. Cheng, H. Nguyen, M. Zhang, D. H. S. Tan, T. A. Wynn, E. A. Wu, J.-M. Doux, T. Wu, L. Ma, G. E. Sterbinsky, M. S. D'Souza, S. P. Ong

and Y. S. Meng, *ACS Appl. Mater. Interfaces*, 2019, **11**, 43138–43145.
31 J. A. Dawson, P. Canepa, M. J. Clarke, T. Famprikis, D. Ghosh and M. S. Islam, *Chem. Mater.*, 2019, **31**, 5296–5304.
32 D. O. Shin, K. Oh, K. M. Kim, K.-Y. Park, B. Lee, Y.-G. Lee and K. Kang, *Sci. Rep.*, 2015, **5**, 18053.
33 Z. Liu, F. Huang, Z. Cao, J. Yang, M. Liu and Y. Wang, *Mater. Lett.*, 2008, **62**, 1366–1368.
34 M. Falco, S. Ferrari, G. B. Appetecchi and C. Gerbaldi, *Mol. Syst. Des. Eng.*, 2019, **4**, 850–871.
35 Y. J. Nam, D. Y. Oh, S. H. Jung and Y. S. Jung, *J. Power Sources*, 2018, **375**, 93–101.
36 J. W. Choi and D. Aurbach, *Nat. Rev. Mater.*, 2016, **1**, 1–16.
37 A. Sakuda, K. Kuratani, M. Yamamoto, M. Takahashi, T. Takeuchi and H. Kobayashi, *J. Electrochem. Soc.*, 2017, **164**, A2474–A2478.